EFFECT OF CAPILLARY, VISCOUS AND GRAVITY FORCES ON GAS CONDENSATE MOBILITY

O.Vizika and F. Kalaydjian

Institut Français du Pétrole, Rueil-Malmaison, France

ABSTRACT

The dependence of the gas and condensate relative permeabilities and of the critical condensate saturation on the fluid properties (interfacial tensions, densities, and wetting characteristics), the rock structure and the operational parameters (velocity) is still poorly captured by the reservoir simulators. In the present paper a model is proposed based on the dependence of *Kr* and condensate mobility on two dimensionless numbers: the capillary number (ratio of the viscous to capillary forces) and the Bond number (ratio of the gravity to capillary forces). The spreading characteristics of the condensate on the substrate (solid surface or water film) are also taken into account. The model is tested against experimental results reported in the literature. A very good agreement is obtained indicating that the model captures correctly most of the controlling parameters.

INTRODUCTION

Describing flow processes that occur both far from and close to the wellbore region is a major issue to accurately predict gas-condensate reservoir performance. When producing a gas condensate reservoir, the pressure draw-down leads to the build-up of a liquid bank which gets progressively mobile. Once mobile, this oil bank flows towards the producing wells that may thus experience impairment. The liquid accumulation that occurs in the vicinity of the production wells tends to lower the deliverability of the gas by multiphase flow effects (*Kr*). In addition to that, the gas which is to be produced, tends to become lighter due to condensation and therefore less marketable.

Predicting a gas condensate reservoir performance requires an accurate modeling of the flow behavior coupled with a correct thermodynamic modeling of the various processes. Once the liquid segregates, the way the densities of the two phases start diverging and the gas/liquid interfacial tension builds up depends on the thermodynamic properties of the gas condensate system. Hence, depending on how close to the critical point the system will get when the pressure decreases and the phase envelope is reached, the liquid accumulation and production is ruled by the balance between three main mechanisms: gravity segregation, capillary hold up and viscous drag. In order to be able to predict gas deliverability, two major features have to be studied: the dependence of K_r on the gas-condensate interfacial tension on one side and on the flow conditions on the other.

For a long time only the effect of interfacial tension on K_r has been studied, and *Kr* changes have been attributed to rapid interfacial tension changes near to the critical point[1,3,9]. More recently the effect of flow velocity on *Kr* has been acknowledged [10,11]. The investigations have been oriented toward a dependence of *Kr* on the capillary number, a dimensionless number that includes both the interfacial tension and the velocity [21,11,12,5].

Another parameter that has been extensively studied is the critical condensate saturation, S_{cc}. There is quite a controversy about the determination of this value. Values ranging between zero and 50% PV have been reported [4,16]. This saturation is the minimum liquid saturation above which the condensate starts being mobile, corresponding thus to a non-zero condensate relative permeability. These low values of the condensate *Kr* control the gas-condensate segregation and impact the phase distribution and the condensate ring buildup. To correctly predict gravity segregation for near-critical systems it is necessary to compare viscous, capillary and gravity forces. To this end two relevant dimensionless numbers are used: the capillary number (Ca, ratio of the viscous to the capillary forces and predominant close to the well) and the Bond number (Bo, ratio of the gravity to the capillary forces and predominant far from the well). More specifically, three configurations can be identified: **1/** near wellbore region : high velocity, high interfacial tension (high Ca, low Bo) ; **2/** reservoir : low velocity, intermediate interfacial tension (low Ca, high Bo) ; **3/** near-critical reservoir : low velocity, low interfacial tension (high Ca, high Bo).

The wetting behavior of condensate on the water phase is a key factor. Complete wetting of the condensate on water would favor hydraulic continuity leading to very low liquid saturations. There is evidence that for near-critical systems the condensate phase perfectly wets either the rock or the water phase covering the pore surface[20]. However, as the pressure decreases towards to the well a wetting transition may occur which would render the condensate phase only partially wetting on water. This would favor its trapping by capillary forces.

The objective of this paper is to present a model for gas condensate K_r as a function of the capillary number and to demonstrate that apparently contradictory laboratory results on the dependence on interfacial tension and flow rate, separately considered, can be reconciled. This is achieved, within the framework of the Darcy description of multiphase flow in porous media (relatively far from the well so that inertial effects are not an issue), by introducing a unique dependence of K_r on the capillary number. Also a modeling of the combined effect of gravity and capillary forces on the critical condensate saturation is introduced. It takes into account the spreading characteristics of the condensate on the substrate (solid surface or water film).

RELATIVE PERMEABILITY AND CAPILLARY NUMBER

As seen in the previous section, the interfacial tension alone cannot adequately parameterize the relative permeabilities. The displacement of several phases in a porous medium is governed by two different forces: viscous and capillary (in the absence of gravity). Capillary pressure is assumed to represent the effect of capillary forces whereas viscous forces intervene in the Darcy equations and are represented by the K_r. Phase distribution and displacement within the porous medium depend on a complex combination of those two forces. K_r was found to depend on interfacial tension[1,3,9], a typical capillary parameter, and on the flow velocity[11]. When the interfacial tension vanishes, the capillary resistance to flow decreases. Therefore, the curvature of the *Kr* curves, that expresses for a given fluid the capillary effect induced by the presence of another fluid, decreases as well. *Kr* become straight lines either when miscibility is approached or when flow-rate is increased enough to make capillary forces negligible. Therefore it is anticipated that K_r depend on the capillary number, *Ca*, a dimensionless number defined as the ratio of the viscous to the capillary forces:

$$Ca = \frac{\mu v}{\sigma} \qquad (1)$$

Dullien (1992) proposed another capillary number that includes the characteristics of the porous medium in addition to those of the fluids:

$$CA = 4\ \frac{Ca.l}{R} \quad (2)$$

where l is the core length and R is a typical size of a pore radius. It is chosen to be equal to the pore size corresponding to the entry pressure deduced from the mercury intrusion curve, that is $R = 2.\sigma.\cos(\theta)/P^*$, with P^* being the pressure at which the mercury starts invading the porous medium. This capillary number is such that when it is equal to unity viscous forces balance capillary forces. When $CA \geq 1$ viscous forces are dominant.

It is worth checking this assumption by comparison with Bardon and Longeron's data (1980). These authors report a significative change in K_r for an interfacial tension smaller than 0.04 mN/m. The tests were carried out in a 40 cm long Fontainebleau sandstone with 82 mD permeability and approximately 10% porosity. The velocity was about 20 cm/h. According to the authors, the Kr curves shape did change for a capillary number equal to 0.4 10^{-4} (standard formulation). To calculate the value of the capillary number CA, it is necessary to know the pore size corresponding to the entry pore pressure. This pore size can be calculated using the rough estimate $\sqrt{(8k/\phi)}$, which gives an average value of about 2 microns and thus a pore radius corresponding to the entry pressure of about 10 µm. This gives $CA = 6.4$. This value of CA, greater than unity, is thus consistent with dominant viscous forces that tend to decrease the K_r curves curvature.

Another example is the one found in Henderson et al. (1995). Gas capillary numbers ranging between 0.18E-5 and 0.14E-4 were reported. The experiments were performed on a core 61cm long, of 92mD permeability, 0.198 porosity and an irreducible water saturation of 0.264. This gives $CA>1$ ($1.96<CA<7.86$), and explains why the authors found an effect of the flow rate, and thus of the capillary number on the relative permeabilities inasmuch as all the tests were performed in the domain of dominant viscous forces.

Another example that can be cited here is the work presented by Asar and Handy (1988). Experiments have been performed in a 1ft long Berea sandstone, with 20% porosity and 193mD permeability, for four interfacial tension values ranging from 0.03 to 0.82 mN/m. Even though only the range of the applied pressure drops is given, and calculation of the exact CA for each experiment is not possible, it is seen that CA ranges between 0.5 and ~80. This explains why for the highest interfacial tension (σ=0.82mN/m) capillary effects are dominant and the measured K_r approach those obtained for conventional gas-oil flood, while for σ=0.03mN/m viscous effects are dominant and K_r curves approach straight lines.

MODELING OF THE RELATIVE PERMEABILITY (*Kr*) AND THE CRITICAL CONDENSATE SATURATION (S_{CC})

Porous Medium Model

It is well known that the transport properties in a porous medium depend strongly on the pore structure geometry. Several papers proved that sedimentary rocks are one of the most extensive natural fractal systems [14,19]. They demonstrated that the pore volume and the pore-rock interface is fractal over length scales that may range from the nanometer to a few microns and have the same surface fractal dimension D_S. D_S takes values between 2 and 3, where 2 characterizes smooth clay-free rocks, while values close to 3 are characteristic of strongly clayey sandstones.

This fractal dimension can be determined easily from the capillary pressure curve at low wetting phase saturation[6] or using sophisticated measurement methods as the x-ray or neutron scattering techniques[2] improving considerably the measurement accuracy.

The modeling approach proposed here has been inspired by de Gennes paper (1985) on the partial filling of a fractal structure by a wetting fluid[15]. The internal surface of a pore is assumed to be a fractal surface; consequently, a perfectly wetting phase remains always continuous. The isotropic fractal surface is modeled as a bundle of parallel capillary tubes with a fractal cross-section. The cross-section of each tube is constructed by an iterative process, by dividing the half perimeter of a circle in η parts and replacing each part by half a circle (Fig. 1). At each step k of the process, N_k new grooves are created with radius R_k and total cross-section area A_k; these characteristics are given as a function of the initial tube radius R_0 by the following relationships:

$$R_k = R_0 (\pi / \eta)^k \tag{3}$$

$$N_k = \eta^k \tag{4}$$

$$A_k = \frac{1}{2} \pi R_0{}^2 (\pi^2 / \eta)^k \tag{5}$$

It can be easily shown that the perimeter of a section is given by

$$L / L_0 = (R / R_0)^{(1-D_L)} \tag{6}$$

where L_0 is the perimeter of the main tube and D_L is the fractal dimension associated with the perimeter (linear fractal dimension, D_L=D_S-1) given by

$$D_L = \frac{\ln \eta}{\ln \eta / \pi} \tag{7}$$

<u>Capillary Pressure and Relative Permeability</u>

At equilibrium, all tubes with size smaller or equal to R_k, where R_k is given by Laplace's law: $P_c = 2\sigma/R_k$ are occupied by the wetting fluid, and larger tubes by the non-wetting one. Thus, the wetting fluid saturation is given as the surface of the tubes occupied by the wetting phase to the total cross section,

$$S_w = \frac{\sum_k^\infty A_k}{\sum_0^\infty A_k} = \left(\frac{R_k}{R_0} \right)^{(2-D_L)} \tag{8}$$

and the correlation between capillary pressure and wetting phase saturation is given by

$$P_c = \frac{2\sigma}{R_0} S_w{}^{1/(D_L-2)} \tag{9}$$

To simplify calculation of K_r, the grooves are replaced by capillary tubes of the same diameter and parallel to the direction of flow. To calculate K_r, Poiseuille's law is applied in each capillary of the bundle. If the flow rate in a single tube of radius R_k is given by

$$Q_k = -\frac{\pi R_k{}^4}{8\mu} \nabla P \tag{10}$$

then the K_r of the wetting phase, which occupies the smallest tubes, is calculated as

$$K_{rw} = \frac{\sum_{k}^{\infty} Q_k N_k}{\sum_{0}^{\infty} Q_k N_k} = S_w^{\left(D_L - 4 \big/ D_L - 2\right)} \tag{11}$$

It has been considered here that the wetting fluid flows down to zero saturation and that there is no irreducible or immobile wetting phase saturation. However irreducible phase saturation can be easily introduced in the calculations as presented elsewhere[23]. This model, when applied to film flow and low wetting phase saturations, permits to estimate K_r for a range of saturation values where reliable experimental results are hard to obtain [13, 17].

Modeling of Gas Condensate Relative Permeability as a Function of CA

Threshold Condensate Saturation

It is proposed now to use the model described above to calculate gas condensate K_r and the impact of capillary number on it. There exists experimental evidence that near the critical point the condensate is the wetting phase that spreads spontaneously on the solid surface[24]. During a depletion, and as the pressure goes down, the condensate saturation builds up. As wetting phase, the condensate occupies first the surface roughness and the smallest pores. If *CA* is low ($0<CA<1$), capillary forces will be dominant for the whole range of condensate saturations. If *CA* increases, viscous forces start being important ($CA \sim 1$), and for high *CA* ($CA>>1$) they become dominant.

For a given macroscopic capillary number different flow regimes may exist inside the porous medium at the pore level. In the bundle of capillaries for example, all tubes are subject to the same pressure gradient. Locally however different flow velocities develop depending on the tube radius. These different velocities lead to different local capillary numbers, meaning that at the same time in the smallest pores flow may be capillary dominated whilst viscous dominated in the rest. That means that for a given macroscopic or bulk capillary number, CA_0, we can define a threshold condensate saturation, S_{tc}, below which flow is capillary dominated and above which viscous forces predominate. Suppose that in the bundle of capillaries model S_{tc} occupies the smallest pores from R_∞ to R_k. The capillary number in the tubes k is CA_k. From the definition of *CA* (Eq.2) it is seen that

$$\frac{CA_k}{CA_0} = \frac{R_k}{R_0} \tag{12}$$

which can be combined to Eq. 8 to express in a different way the wetting fluid saturation

$$S_c = \left(\frac{CA_k}{CA_0}\right)^{(2-D_L)} \tag{13}$$

It is now obvious that the threshold condensate saturation is the one for which $CA_k = 1$.

$$S_{tc} = (CA_0)^{(D_L-2)} \tag{14}$$

This expression permits to calculate for a given pore structure (given D_L) the part of the wetting fluid flowing by capillary dominated flow as a function of the macroscopic capillary number. Fig. 2 shows the dependence of S_{tc} on *CA* for different fractal dimensions. It is seen that the higher the capillary number the lower the threshold condensate saturation. It is also seen that, for a given *CA*, S_{tc} increases with D_L. This means that, for the same macroscopic flow conditions, the more fractal the pore structure the higher the wetting phase saturation (condensate) subject to a capillary flow regime. In other words in a clayey sandstone (high D_L) the wetting phase maintains a low mobility up to rather high saturations, even at high capillary numbers where viscous forces would be expected to predominate.

Condensate Relative Permeability

The wetting fluid *Kr* is given by Eq. 11 up to S_{tc}. The fluid above the threshold saturation, S_{tc}, flows in the larger tubes by viscous dominated flow. The respective relative permeability for $S_c > S_{tc}$ is taken proportional to the flowing saturation (straight lines).

A sample calculation of the condensate (wetting phase) K_r and its evolution with *CA* is given in Fig. 3. A D_L = 1.4 has been used in these calculations. This value is representative of a very weakly clayey sandstone. The K_{rc} curves for three different capillary numbers (*CA*=3, 10, 100) are presented in this figure. For comparison purposes the curve for purely capillary dominated displacement is also given. It is seen that as viscous forces become important (increasing *CA*) the part of the fluid flowing under capillary dominated flow is reduced, and *Kr* increases considerably.

Gas Relative Permeability

Gas as the non-wetting phase occupies the bulk of the pores. In order to calculate its relative permeability, it is assumed that, if the condensate occupies all tubes with radius smaller than R_k, gas flows like in a single pore with radius $R_g=R_0+R_1+\ldots+R_k$ (Moulu et al., 1997). Thus for low condensate saturations ($S_c<S_{tc}$), *Krg* is given by

$$K_{rg} = K_{rg\,\max}\left(1 - S_c{}^{1/(2-D_L)}\right)^4 \tag{15}$$

K_{rgmax} is the maximum value of the gas K_r in presence of the other phase. For lower S_g, ($S_c>S_{tc}$), gas circulates in the biggest pores with a K_{rg} proportional to the flowing gas saturation

$$K_{rg} = \frac{S_g}{1-S_{tc}} K_{rg}(S_{tc}) \tag{16}$$

It is seen that, as well as K_{rc}, K_{rg} depends on the porous medium (through D_L) and on the capillary number (through the dependence on S_{tc}).

A sample calculation of the gas (non-wetting phase) relative permeability and its evolution with *CA* is given in Fig. 4. As for K_{rc} (Fig. 3) a linear fractal dimension of 1.4 has been used in these calculations. The K_{rg} curves for three different capillary numbers (*CA*=3, 10, 100) are plotted. Also the curve for purely capillary dominated displacement is given for comparison. As viscous forces increase (increasing *CA*) the S_{tc} decreases and the saturation range where gas permeability is proportional to S_g increases.

Comparison with Experiments

The proposed model is now tested against experimental measurements of near critical fluid K_r as reported in the literature. K_r at near critical conditions have been reported by Schechter and Haynes (1992). The experiments (injections at an average flow rate of 0.098cc/sec, for three interfacial tensions: 0.1, 0.006 and 0.002 mN/m) were performed in a Clashach sandstone of 30cm in length, with a permeability of 200mD and a porosity of 18%. These data permit to calculate the *CA* numbers from the *Ca* values given by the authors: for *Ca* $3x10^{-4}$, $4x10^{-3}$ and 10^{-2} we get the respective *CA* values 12, 133 and 400. Then S_{tc}, K_{rc} and K_{rg} have been calculated with the model by taking D_L equal to 1.65. This value, representative of a clayey sandstone[14], has been measured in a Clashach sample of comparable permeability to the one used in Schechter and Haynes' experiments. The comparison between Schechter's measurements and the present model's predictions are given in Figs 5 and 6. It is seen that for this example a very good agreement between experiment and calculations is obtained. The model successfully predicts gas condensate *Kr* as a function of the macroscopic capillary number. It also successfully predicts the threshold saturation S_{tc}, below which the reduction of condensate mobility becomes significant. It is worth noting that there is no adjustable parameter in the model. The only parameter that has been assigned an arbitrary value (not reported in 21) is the fractal dimension D_L.

Bardon and Longeron (1980) have also reported K_r measurements at different and very low interfacial tensions. For flow rates 0.011, 0.01, and 0.012 cc/sec and interfacial tensions 0.065, 0.038, and 0.0014 mN/m respectively, the *Ca* numbers calculated by the authors were: 0.19×10^{-4}, 0.38×10^{-4}, 0.11×10^{-2}.The *CA* numbers calculated as indicated above are 2.5; 6; 168. Comparison between the experiments and the calculations are given in Figs 7 and 8 for the condensate and the gas K_r respectively. The fractal dimension has been taken equal to 1.3. This value is representative of a very weakly clayey sandstone as was the one used in the experiments (Fontainebleau sandstone). A very satisfactory agreement is observed considering the uncertainties in the experimental K_r that have been obtained by numerical fitting of displacement/production data.

Gravity Segregation and Critical Condensate Saturation, S_{cc}

The same model for the porous medium can be used to calculate the critical condensate saturation for mobility as a function of the spreading and interfacial properties of the fluid system, and the characteristics of the pore structure. We need first to introduce the Bond number, which is defined as the ratio of the gravity to capillary forces, in a way equivalent to the one proposed by Schechter et al. (1994) (e.g. defined at the macroscopic scale).

$$Bo = \frac{\Delta \rho g R l}{\sigma} \tag{17}$$

It is considered here that S_{cc} is the minimum saturation at which the condensate is continuous and the conditions are such that gravity forces, favoring segregation, are dominant over the capillary forces that favor condensate trapping. That means that the condensate has first to form continuous films on the solid substrate or on the water, if interstitial water is present in the porous medium. Still these continuous films may be immobile if gravity forces are not strong enough compared to capillarity. S_{cc} is the saturation above which the condensate K_r takes a non-zero value. It is to be distinguished from the threshold condensate saturation, S_{tc}, that determines the saturation below which the condensate has a reduced though finite mobility.

In a water-wet porous medium, in presence of irreducible water saturation, a relevant parameter is the spreading coefficient of oil (condensate) on water: $\boldsymbol{S} = \sigma_{wg}-(\sigma_{wc}+\sigma_{cg})$. At equilibrium $\boldsymbol{S}$ is always negative or equal to zero. It has been already verified through numerous studies on three-phase displacement that fluid distributions depend on the sign of the spreading coefficient of oil on water in presence of gas. For $\boldsymbol{S} = 0$, oil (condensate) forms a film spontaneously on water in presence of gas. Spreading oil films assure hydraulic continuity of the oleic phase and can lead to very high recoveries. For $\boldsymbol{S} < 0$, oil does not spread on water in presence of gas and a finite contact angle, θ, is formed between the gas-condensate and water-condensate interfaces. The above hold rigorously only for a flat solid surface. Wetting on a rough surface is very different, and apparent contact angles depend both on the wetting properties of the flat surface and on the structure of the roughness[18]. Two types of trapping can be considered: a) continuous phase trapping in the smallest tubes where capillary forces are very strong and b) discontinuous phase trapping, when $\boldsymbol{S} < 0$ and the condensate is in disconnected form.

Spreading Condensate Trapping (S=0)

In absence of water or if the condensate spreads on the water ($\boldsymbol{S}$=0) films are spontaneously formed at the moment of condensate apparition. These films assure automatically hydraulic continuity. The continuous phase trapping is related to the Bond number. In the bundle of capillaries model, introduced in paragraph 3.1, the condensate occupies the smallest pores, from R_∞ to R_k in absence of water or from R_{wi} to R_k , if the tubes from R_∞ to R_{wi} are occupied by irreducible water. The Bond number in the tubes k is Bo_k. From its definition it results

$$\frac{Bo_k}{Bo_0} = \frac{R_k}{R_0} \tag{18}$$

If $Bo_k > 1$ gravity forces predominate and R_k tubes are emptied under gravity segregation. The critical condensate saturation for mobility of a continuous fluid, $S_{cc/c}$, is the one for which $Bo_k=1$ and is given by

$$S_{cc/c} = \left(Bo_0\right)^{(D_L-2)} - S_{wi} \tag{19}$$

Non-spreading Condensate Trapping (S<0)

If $\boldsymbol{S}<0$, in condensate apparition small droplets are formed. If the substrate is flat, these droplets form an angle θ for which

$$\cos\theta = 1 + \frac{S}{\sigma_{cg}} \tag{20}$$

On a fractal surface they form an apparent contact angle, θ_{app}, related to θ with the following expression[18]

$$\cos\theta_{app} = \left(\frac{R_0}{R_k}\right)^{D_L-1} \cos\theta \tag{21}$$

where R_0 and R_k are the upper and the lower limits of fractal behavior. If $\cos\theta_{app} = 1$, the non-spreading condensate ($\cos\theta < 1$) remains continuous. The fractal surface induces wetting of a non-spreading liquid. Thus the criterion for spreading phase mobility has to be applied, as explained above. The critical condensate saturation is given by Eq. 19.

When $\cos\theta_{app} < 1$ the condensate forms lenses and remains disconnected. It is considered that disconnected phase remains immobile and it is not subject to gravity segregation. The critical saturation for discontinuous liquid mobility, $S_{cc/d}$, is the one occupying tubes up to R_k for which $\cos\theta_{app}$ becomes equal to 1. It is given by the following expression as a function of the spreading and interfacial properties of the system and the characteristics of the pore structure here expressed by the fractal dimension D_L.

$$S_{cc/d} = \frac{1}{\pi^{\frac{2-D_L}{D_L-1}}} \left(1 - \left(\cos\theta\right)^{2-D_L}\right) \tag{22}$$

Then the critical saturation for mobility of a non-spreading condensate is the sum of the trapped continuous (if any) and trapped discontinuous liquid.

Fig. 9 shows the critical condensate saturation for a discontinuous phase ($\boldsymbol{S}$<0, $cos\theta_{app}$<1) for various values of the fractal dimension. $S_{cc/d}$ can take extremely high values for strongly non-spreading fluids (θ=90°, cosθ=0)) and highly fractal pore space (high D_L).

CONCLUSIONS

Flow rate and interfacial tension dependence of relative permeability is explained on the basis of the competition between capillary and viscous forces. K_r are shown to deform and approach straight lines when viscous forces overcome capillary forces. This can be achieved either by decreasing the interfacial tension or increasing the flow rate. To account for that, a capillary number, *CA*, introduced by Dullien[8] is used. It includes, in addition to fluid properties, porous medium properties. *CA* allows to precisely define the flow rate (or interfacial tension) threshold above (respectively below) which K_r start to deform. This hypothesis has been validated on experimental results obtained either by modifying the interfacial tension or the flow rate.

A model has been proposed to calculate gas condensate K_r as functions of the capillary number. The model includes the structure characteristics of the porous medium through its fractal dimension. It predicts the modification of the K_r curves as the capillary number changes (velocity or interfacial tension changes). The model has been tested against experimental results reported in the literature and a very satisfying agreement has been obtained.

A threshold condensate saturation, S_{tc}, can be predicted below which the condensate mobility is extremely reduced, even though finite. S_{tc} may be very high in highly fractal (very clayey) sandstones. It decreases with increasing capillary number.

The critical saturation for condensate mobility, S_{cc}, increases with increasing interfacial tension (decreasing Bond number) and fractal dimension. Non-spreading condensate would be subject to severe trapping, increasing with increasing fractal dimension and decreasing spreading coefficient.

NOMENCLATURE

A_k = area of the grooves of step k
Ca = standard capillary number (=$\mu v/\sigma$)
CA = Capillary number (=$4Ca\ l/R$)
Bo = Bond number (= $\Delta\rho gRl/\sigma$)
D_L = linear fractal dimension
D_S = surface fractal dimension
g = acceleration of gravity
k = permeability
K_r = relative permeability
K_{ri} = relative permeability of fluid i
K_{rgmax} = maximum gas relative permeability
l = porous medium length
L = perimeter of a section of the fractal object
N_k = number of objects of step k
P_c = capillary pressure
Q_k = flow rate in tube of radius R_k
R = entry pore size
R_0 = initial capillary tube radius in the fractal pore model
R_i = capillary radius (i= 1,2,...k step of the fractal construction)
R_g = radius for gas flow in the fractal pore model
R_{wi} = maximum tube radius occupied by irreducible water
S = saturation
$\boldsymbol{S}$ = spreading coefficient
S_i = saturation of fluid i
S_{wi} = irreducible water saturation
S_{cc} = critical condensate saturation
$S_{cc/c}$ = critical condensate saturation for continuous phase
$S_{cc/d}$ = critical condensate saturation for discontinuous phase
S_{tc} = threshold condensate saturation
v = velocity

∇P = pressure gradient
$\Delta\rho$ = density difference
η = number of new tubes created at each step
θ = contact angle between gas-condensate and water-condensate interfaces
μ = viscosity
σ = interfacial tension
ϕ = porosity

Subscripts
c, g, w = condensate, gas, wetting phase

REFERENCES

1. Asar, H., and Handy, L.L., 1988, "Influence of Interfacial Tension on Gas-Oil Relative Permeability in a Gas-Condensate System," *SPE RE*, February, 257.
2. Bale, H.D., Schmidt, P.W., 1984, Phys. Rev. Lett., 53, 596.
3. Bardon, C., and Longeron, D., 1980, "Influence of Very Low Interfacial Tensions on Relative Permeability," *SPE J*, October, 391-401.
4. Barnum, R.S., Brinkman, F.P., Richardson, T.W. and Spillette, A.G., 1995, "Gas Condensate Reservoir Behaviour: Productivity and Recovery Reduction due to Condensation," SPE 30767, SPE Annual Technical Conference and Exhibition, Dallas, TX, October 22-25.
5. Blom, S.M.P., Hagoort, J., Soetekouw, D.P.N., 1997, "Relative Permeability at Near-Critical Conditions," SPE38935, SPE Annual Technical Conference and Exhibition, San Antonio, Texas, October 5-8.
6. Davis, H.T., 1989, "On the Fractal Character of the Porosity of Natural Sandstone," Europhys. Lett., 8(7), 629-632.
7. De Gennes, P.G., 1985, "Partial Filling of a Fractal Structure by a wetting fluid," Physics of Disordered Materials, Adler, Fritzche, Ovshinsky Eds, Plenum Publishing Corporation, 227-241.
8. Dullien, F.A.L.: *Fluid transport and pore structure*, 2nd Edition, Academic Press Inc., 1992.
9. Haniff, M.S., and Ali, J.K., 1990, "Relative Permeability and Low Tension Fluid Flow in Gas Condensate Systems," SPE20917, European Petroleum Conference, The Hague, Netherlands, October 22-24.
10. Henderson, G.D., Danesh, A., Tehrani, D.H., and Peden, J.M., 1993, "An Investigation into the Processes Governing Flow and Recovery in Different Flow Regimes present in Gas-Condensate Reservoirs", SPE26661, SPE Annual Technical Conference and Exhibition, Houston, TX, October 3-6.
11. Henderson, G.D., Danesh, A., Tehrani, D.H., Al-Shaidi, S., and Peden, J.M., 1995, "Measurement and Correlation of Gas Condensate Relative Permeability by the Steady-State Method," SPE30770, SPE Annual Technical Conference and Exhibition, Dallas, TX, Oct. 22-25.
12. Kalaydjian, F. J-M., Bourbiaux, B.J., Lombard, J-M., 1996, "Predicting gas-condensate reservoir performance: how flow parameters are altered when approaching production wells," SPE36715, SPE Annual Technical Conference and Exhibition, Denver, Colorado, October 6-9.
13. Kalaydjian, F.J-M., Moulu, J-C., Vizika, O. and Munkerud, P-K., 1997, "Three-phase flow in water-wet porous media : gas/oil relative permeabilities for various spreading conditions," J. Petr. Sci. Eng., 17, 275-290.
14. Katz, A.J., Thompson, A.H., 1985, "Fractal Sandstone Pores: Implications for Conductivity and Pore Formation," Phys. Rev. Lett, 54(12), 1325-1328.
15. Lenormand, R., 1990, "Gravity-assisted inert gas injection: micromodel experiments and model based on fractal roughness," The European Oil and Gas Conference, Altavilla Milica, Palermo, Sicily, October 9-12.

16. Morel, D.C., Lomer, J.-F., Morineau, Y.M., and Putz, A.G., 1992, "Mobility of Hydrocarbon Liquids in Gas Condensate Reservoirs: Interpretation of Depletion Laboratory Experiments," SPE24939, SPE Annual Technical Conference and Exhibition, Washington, DC, October 4-7.
17. Moulu, J.C., Vizika, O., Kalaydjian, F., Duquerroix, J-P., 1997, "A New Model for Three-Phase Relative Permeabilities Based on a Fractal Representation of the Porous Medium," SPE38891, SPE Annual Technical Conference and Exhibition, San Antonio, Texas, October 5-8.
18. Onda, T., Shibuichi, S., Satoh, N., Tsujii, K., 1996, "Super-Water-Repellent Fractal Surfaces," Langmuir, 12(9), 2125-2127.
19. Radlinski A.P., Radlinska, E.Z., Agamalian, M. Wingall, G.D., Lindner, P., Randl, O.G., 1999, "Fractal Geometry of Rocks," Phys. Rev. Lett, 82(15), 3078-3081.
20. Ragil, K., Bonn, D., Broseta, D., Indekeu, J., Kalaydjian, F., Meunier, J.: "The Wetting Behavior of Alkanes on Water," *J. Petr. Sci. Eng.,* 1998, 20, 177-183.
21. Schechter, D.S., Haynes, J.M., 1992, "Relative Permeabilities of a Near Critical Binary Fluid," Transport in Porous Media, 9, 241-260.
22. Schechter, D.S., Zhou, D., Orr, Jr., F.M. 1994, "Low IFT drainage and imbibition," J. Petr. Sci. Eng., 11, 283-300.
23. Vizika, O., 1993, "Effect of the Spreading Coefficient on the Efficiency of Oil Recovery with Gravity Drainage," Symposium on Enhanced Oil Recovery, 205th National Meeting of ACS, Denver CO, March 28 - April 2.
24. Williams, J.K., Dawe, R.A., 1989, "Near-Critical Condensate Fluid Behavior in Porous Media – A Modeling Approach," SPERE, May, 221-227.

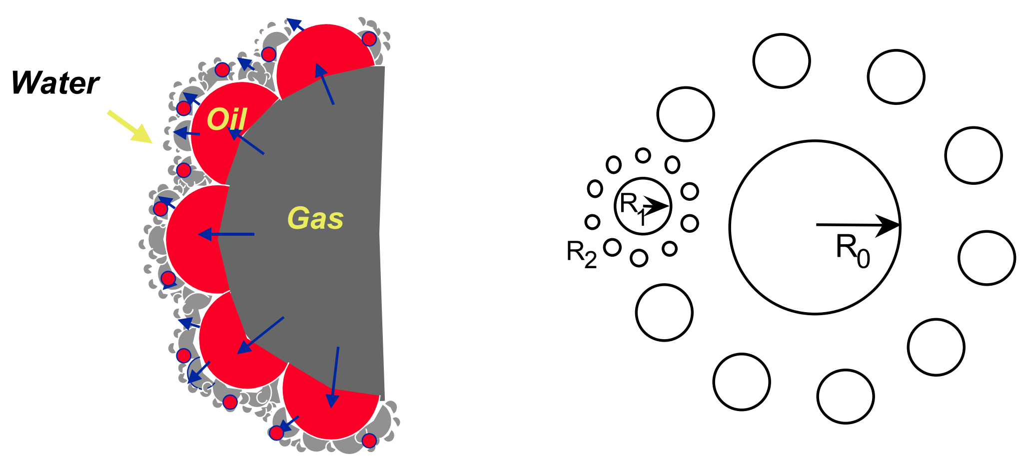

Figure 1. The fractal pore model and the phase distribution within it.

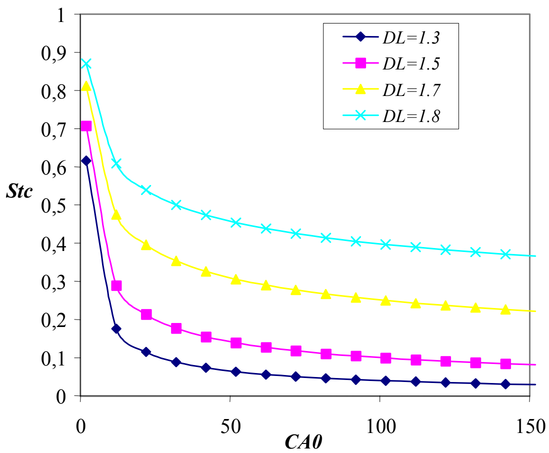

Figure 2. Threshold condensate saturation as a function of the macroscopic capillary number for various fractal dimensions

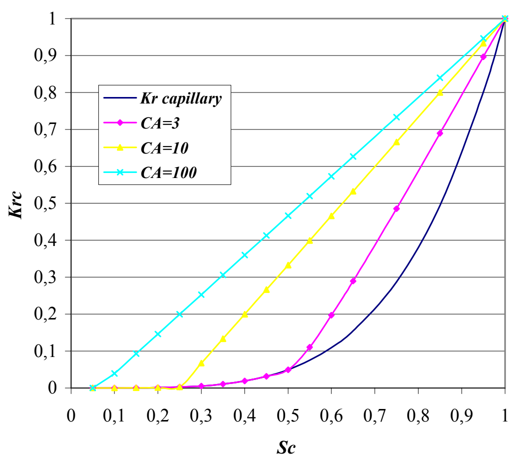

Figure 3. Effect of capillary number on the condensate relative permeability (D_L=1.4)

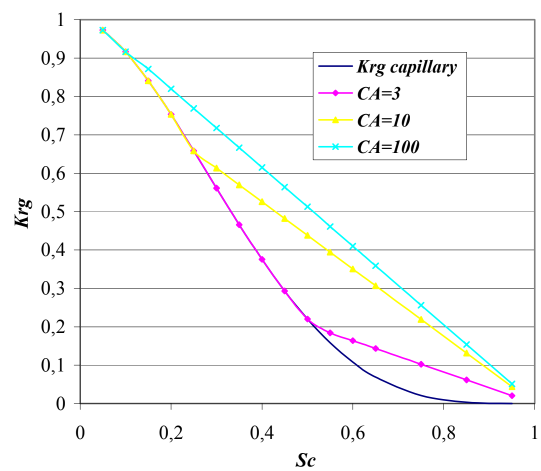

Figure 4. Effect of capillary number on the gas relative permeability (D_L=1.4)

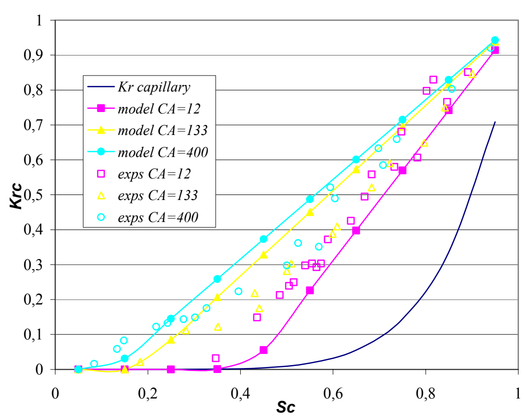

Figure 5. K_{rc}: Comparison between the model and Schechter and Haynes' experimental results

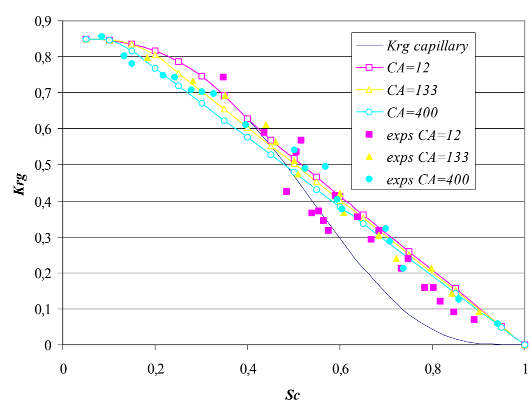

Figure 6. K_{rg}: Comparison between the model and Schechter and Haynes' experimental results

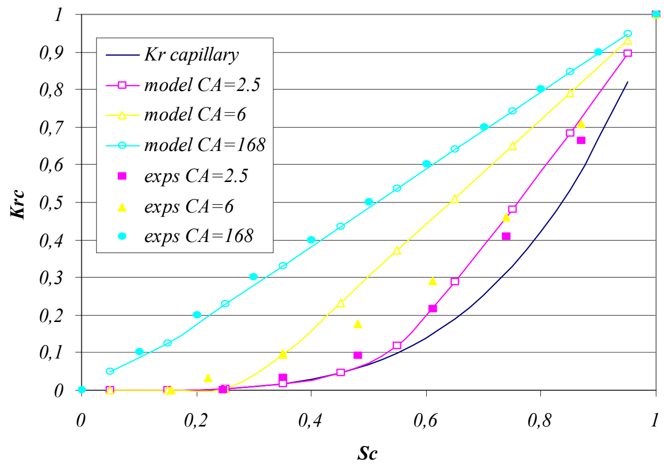

Figure 7. K_{rc}: Comparison between the model and Bardon and Longeron's experimental results

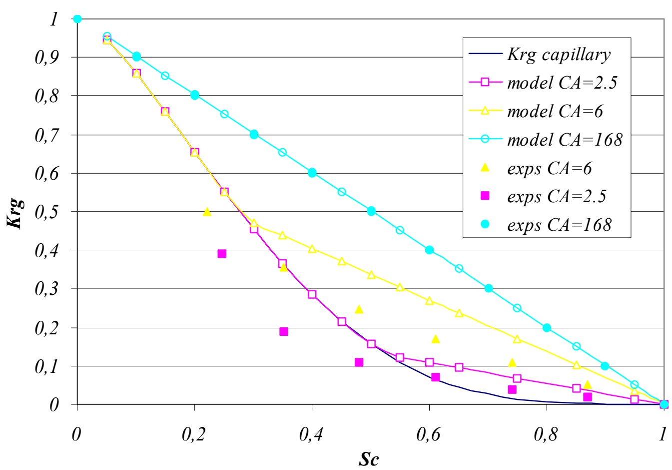

Figure 8. K_{rg}: Comparison between the model and Bardon and Longeron's experimental results

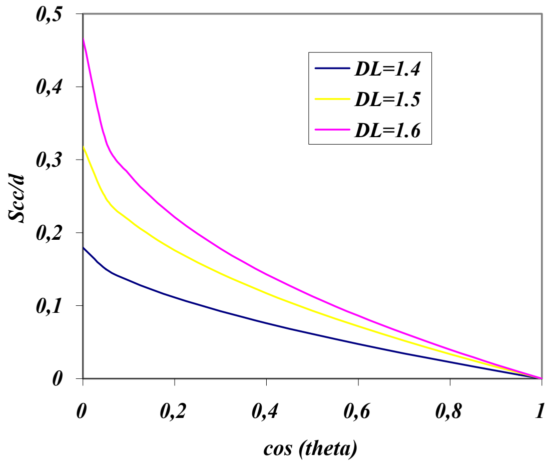

Figure 9. K_{rg}: Effect of $\cos\theta$ (negative spreading coefficient) on the critical condensate saturation of a discontinuous phase for various values of the fractal dimension